Polymer 50 (2009) 721–727

Contents lists available at ScienceDirect

Polymer

journal homepage: www.elsevier.com/locate/polymer

Cooperative surface-induced self-assembly of symmetric diblock copolymers confined films with embedded nanorods

Linli He [a], Linxi Zhang [b,*], Haojun Liang [c]

[a] Department of Physics, Zhejiang University, Hangzhou 310027, PR China
[b] Department of Physics, Wenzhou University, Wenzhou 325027, PR China
[c] Department of Polymer Science and Engineering, University of Science and Technology of China, Hefei, Anhui 230026, PR China

ARTICLE INFO

Article history:
Received 14 August 2008
Received in revised form
9 November 2008
Accepted 23 November 2008
Available online 30 November 2008

Keywords:
Self-consistent field theory
Self-assembly
Nanorod

ABSTRACT

The self-assembly of symmetric diblock copolymers confined films with embedded nanorods is investigated by the self-consistent field (SCF) theory. We obtain some phase diagrams as a function of film thickness H and nanorod diameter D. The increase in preferential nanorod diameter D can promote the formation of incomplete cylindrical and spherical structures near the film surfaces, and can also induce complete lamellar, cylindrical and spherical structures in the interior. The formation of these induced self-assembled structures is due to the competition between inner surface confinement (two parallel surfaces) and outer surface confinement (nanorods). This investigation can provide some insights into the self-assembly of diblock copolymers with complex confinements.

1. Introduction

One of the most fascinating properties of diblock copolymers (DBCPs) is their ability to self-assemble into various ordered microstructures, and these structures depend on the relative length of the blocks, the molecular weight, and the interaction parameter between the blocks [1,2]. These ordered bulk microstructures include lamellae (H), bicontinuous gyroid (G), hexagonally packed cylinders (C), and closed-packed spheres (CPS) [3]. Materials with various ordered structures have promised for application toward the design of diversified nanodevices such as photonic crystals [4,5]. Therefore, recent research has explored various additional external influences on self-assembly of block copolymers, such as surface confinement [6–8], templating by surface patterns [7,9], shear [10–12] and electric fields [13–15]. The effects of surface confinement on self-assembly of DBCPs have received tremendous attentions for various confinement surfaces, including one-dimensional (substrate and two parallel surfaces) [16–24], two-dimensional (cylindrical surface) [25–35] and three-dimensional (spherical surface) [27,29,36,37] confinements. When the DBCPs are confined to physically or chemically defined surfaces, besides the pertinent factors applying to ordering in bulk samples, the polymer–surface interactions and confined geometry exhibit great influences on the self-assembled morphologies, which will be extremely different from those observed in the bulk. Therefore, introducing a surface confinement into the DBCPs system is proven to be another efficient method to explore the novel morphologies of DBCPs [38].

Many experimental [39–41], theoretical [42–45], and computer simulation [24,46,47] studies of the microstructure of symmetric DBCPs confined films (one-dimensional confinement) have been carried out in the last decades. By finely tuning the polymer–surface interactions and confinement geometry, one can achieve molecular-level process to control the self-assembly of polymers, and can also obtain much richer morphologies such as hybrid structures. Recent studies have also used a variety of simulation techniques to investigate the effects of nanoparticles (NPs) dispersed in complex fluids such as block copolymers [3,48–55] on self-assembly of block copolymers. The NPs are another external influence on self-assembly of block copolymers, which can be regarded as an outer surface confinement for polymers, and can provide a different type of confinement surface from those inner confinement surface mentioned above. The physical and chemical properties of embedded NPs significantly affect the final morphologies of block copolymers. For example, recently, we extended this concept to investigate the effects of spherical NPs on the lamellar phase separation of diblock copolymers [56]. Meanwhile, the NPs can be produced with a wide range of shapes, including sphere, rod, branched rod, cube, and pyramid. Especially, nanorods (NRs) are interesting for photovoltaic

* Corresponding author. Tel.: +86 571 88483790; fax: +86 571 87951328.
E-mail address: lxzhang@zju.edu.cn (L. Zhang).

0032-3861/$ – see front matter © 2008 Elsevier Ltd. All rights reserved.
doi:10.1016/j.polymer.2008.11.042

applications since the long axis of the rod provides a continuous channel for transporting electrons, an advantage over spherical nanoparticles. A large increase of interest has been focused on suspended NRs used to direct nanoscale block copolymer assembly [57–62].

Buxton et al. used simulations to show that NRs partitioning into the minority phase of a polymer blend could result in a bicontinuous morphology with a percolated network of NRs and enhanced mechanical properties [57]. Laicer and co-workers also experimentally examined the impacts of Au nanorods on self-assembly of polystyrene-*block*-polyisoprene (PS-*b*-PI) copolymer solution [58]. Their results show that Au nanorods act as morphological seeds that specifically template the growth and direction of copolymer cylindrical-phase domains. Additionally, they also investigated the effects of nanorod diameter and polymer–surface interactions on the morphology [59]. They found that selective interactions between either PS or PI block and the nanorod surface are sufficient to template the organization of the surrounding cylindrical mesophase, and that a wide range of nanorod diameters can successfully seed cylinder-phase domains.

Several researchers have respectively investigated the effects of inner surface confinement (e.g. parallel surfaces) and outer surface confinement (e.g. nanoparticles) on self-assembly of nanoparticles. Marco et al. investigated morphologies of DBCPs confined in-between two concentric spheres with radii R_1 and R_2, where the inner sphere models the surface of nanoparticle and the outer sphere models the free surface of diblock copolymer film [60]. The obtained structures include: parallel, perpendicular, mixed and perforated lamellae, parallel and perpendicular cylinders and spheres. Their simulation suggests that novel nanostructures can be guided by combining with various types of surface confinements. Although the shapes of the inner and the outer surface confinements are all sphere in their model, some special morphologies are obtained [60]. If the shapes of inner surfaces are different from the outer ones, it may self-assemble into some new ordered microstructures. Here, we employ the self-consistent field (SCF) method to study cooperative surface-induced self-assembly of symmetric diblock copolymers confined films with the embedded nanorods. Different polymer-surface interactions, film thicknesses, and nanorod diameters are considered.

2. Theory and model

In this report, we discuss cooperative inducement from inner and outer surface confinements to self-assembly of symmetric DBCPs, which can form a lamellar phase (L) in the bulk with the period of lamella L_0. Two cases are considered here: one nanorod and two nanorods are embedded with the distance of the period of lamella L_0, see Fig. 1. The top and bottom parallel surfaces model inner surface confinement, and NRs model outer surface confinement, respectively.

We choose the repeat box with the size of $L_x \times L_y \times H$ to match the characteristic period of bulk lamella L_0, here $L_x = L_0$, and $L_y = 2L_0$. In our study, the top and bottom surfaces are neutral and unpenetrable, and periodic boundary conditions are imposed in the x and y directions. The NRs with infinite length are arranged periodically along the y-direction, and the positions in the z-direction are $0.5H$ for one nanorod case, see Fig. 1(a) and (b), and $0.25H$ and $0.75H$ for two nanorods case, see Fig. 1(c) and (d).

For the DBCPs with surface confinement, the self-consistent field theory free energy per chain in the unit of k_BT has the form:

$$F = -\ln\left(\frac{Q}{V}\right) + \frac{1}{V}\int \mathrm{d}r[\chi_{AB}N\phi_A\phi_B - \omega_A\phi_A - \omega_B\phi_B + h_{NA}\phi_A + h_{NB}\phi_B - P(\phi_0 - \phi_A - \phi_B)] \quad (1)$$

In this expression, ϕ_A and ϕ_B are the monomer densities, and $\phi_0 = \phi_A + \phi_B$ is the total monomer density. The single-chain partition function $Q = \int \mathrm{d}r\, q(r,1)$ is the partition function of a single diblock copolymer chain in the mean fields, ω_A and ω_B. These mean fields are in turn produced by the surrounding chains. The end-segment distribution function q (r, s) gives the probability that a chain segment of contour length S and containing a free chain end has its "connected end" located at r. The function q (r, s) and its conjugate q' (r, s) satisfy the modified diffusion equations:

$$\frac{\partial}{\partial s}q(r,s) = R_g^2\nabla^2 q(r,s) - N\omega q(r,s) \quad (2)$$

$$-\frac{\partial}{\partial s}q'(r,s) = R_g^2\nabla^2 q'(r,s) - N\omega q'(r,s) \quad (3)$$

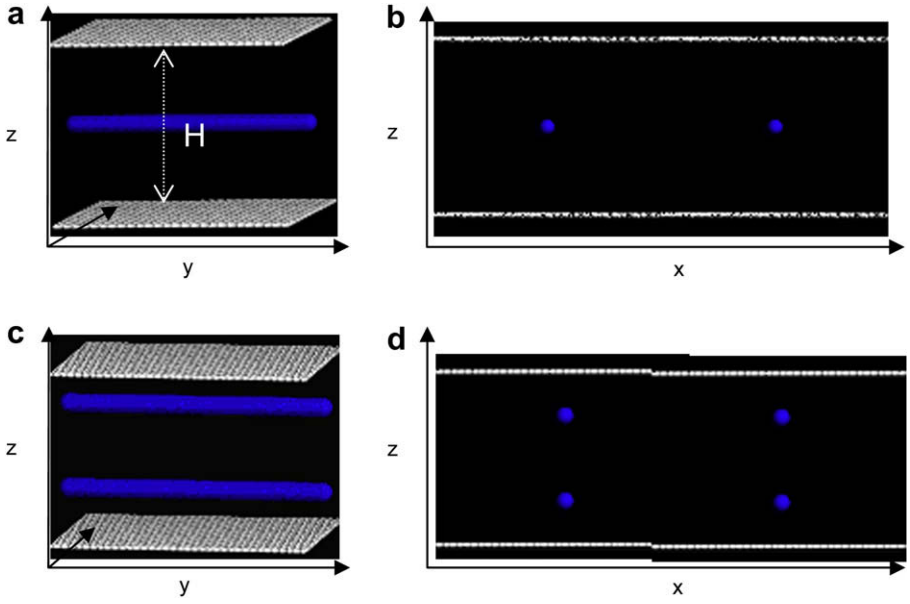

Fig. 1. Configurations for confined films with embedded one (a) or two NRs (c). Here the diameter of nanorod is D, and the distance between two successive NRs in the x direction is L_0, see (b), and (d). The film thickness is H. One NR is located at $0.5H$, and two NRs are located at $0.25H$ and $0.75H$ in the z-direction.

with the initial conditions $q(r, 0) = 1$ and $\hat{q}(r, 0) = 1$. Here, R_g is the radius of gyration for an ideal Gaussian chain. For $0 \le s \le f_A$, $\omega = \omega_A$ and $f_A \le s \le 1$, $\omega = \omega_B$. We use the Crank–Nicholson scheme in solving the modified diffusion equations. In Eq. (1), h_{NA} and h_{NB} represent the surface fields that the outer surface of nanorods acts on, namely, A or B monomer, respectively. P is a Lagrange multiplier (as a pressure) to ensure the incompressibility condition. Minimization of the free energy with respect to the densities and mean fields leads to the following SCFT equations:

$$\omega_A(r) = \chi_{AB}(\phi_B(r) - f_B) + U_A(r) + P(r) \quad (4)$$

$$\omega_B(r) = \chi_{AB}(\phi_A(r) - f_A) + U_B(r) + P(r) \quad (5)$$

$$\phi_A(r) = \frac{V}{Q}\int_0^{f_A} ds q(r,s)q'(r,s) \quad (6)$$

$$\phi_B(r) = \frac{V}{Q}\int_{f_A}^{1} ds q(r,s)q'(r,s) \quad (7)$$

These equations can be solved self-consistently. For simplicity, the polymer-surface interaction potential is assumed to be short-ranged, and it is represented by contact interactions:

$$h_{NA(B)} = \begin{cases} U_{NA(B)} & \text{on the lattice next to the nanorods} \\ 0 & \text{bulk} \end{cases} \quad (8)$$

where $U_{NA(B)}$ is the strength of the surface field. In this study, two types of outer surfaces of NRs are considered: (a) neutral surface, for which the outer surface of NRs has no preference to the blocks ($U_{NA} = 0$ and $U_{NA} = 0$); (b) strongly A-attractive surface, for which the outer surface of NRs energetically prefers the A blocks ($U_{NA} = -60$ and $U_{NB} = 0$). In order to present the fact that the polymer densities should approach zero at the confinement surface, the incompressibility condition is modified, such that $\phi_A(r) + \phi_B(r) = \phi_0(r)$, where $\phi_0(r)$ is chosen to be 0.5 on the lattices next to the surfaces and 1 everywhere else. On the surface sites of the confinement, the end-segment distribution functions and polymer densities are set to zero. In our calculations, we take $0.2R_g$ as the lattice size. We calculate the characteristic period of bulk lamella L_0 for symmetric DBCPs, namely, $L_0 = 4.4R_g$. Meanwhile, the free energies are run for several times using different random initial mean fields ω_A and ω_B to ensure that the exact equilibrium morphology has been obtained. Moreover, two sequential iteration steps are compared to determine the stable ones until the difference between them is less than 1×10^{-12} (in the unit of k_BT). The very stable morphology is obtained after long iteration steps.

3. Results and discussion

In this section, we present the results for symmetric DBCPs confined in two parallel neutral surfaces with embedded one or two NRs. Our main aim is to investigate the morphologies of mixtures (copolymers/nanorods) for various film thicknesses H and nanorod diameters D, and further to explore the cooperative inducement of both inner surface confinement of two parallel surfaces and outer surface confinement of NRs to self-assembly of DBCPs.

3.1. One nanorod

First we present the morphologies of symmetric DBCPs confined films embedded with one neutral NR. As shown in Fig. 2, the perpendicular lamellae ($L_\perp$) of the melt are observed without NR (i.e., $D/L_0 = 0$, see Fig. 2(a1) and (b1)), which is in full agreement with the results from experiments [41], theories [44], and simulations [47]. For the two cases with film thicknesses $H/L_0 = 2.0$ and $H/L_0 = 3.0$, with the increase in nanorod diameter D/L_0, we observe that the neutral NR has almost no effect on the perpendicular lamellae ($L_\perp$) of symmetric DBCPs confined films.

By contrast, in the case of A-attractive NR the situation is different. Due to the adsorption of nanorod to A block, the central nanorod surrounded by a "coating" consisting of A block always forms a cylinder denoted by C'. Meanwhile, besides the central cylinders (C'), some induced structures are also observed in Fig. 3, which cannot be observed in neat symmetric DBCPs confined films. For the cases of $H/L_0 = 1.0$ and $H/L_0 = 2.0$, when the value of D/L_0 increases from 0.09 to 1.0 in step of 0.09, a series of integrated morphologies of mixtures are denoted as $C_{1/2} + C'$, $S_{1/2} + C'$, $L_\parallel + C'$, $C_{1/2}$, and $L_\parallel + C'$, $C_{1/2} + C'$, $S_{1/2} + C'$, C'. For the case of $H/L_0 = 3.0$, the morphologies of mixtures are respectively $C + C'$ and $L_\parallel + C'$. Except for the central cylinders (C'), these induced structures also include $C_{1/2}$ (a2, b3 and c2), $S_{1/2}$ (a3, b4) and $L_\parallel$ (a4, b2 and c3), where C, S and $L_\parallel$ represent the structures of cylinder, sphere and parallel lamellae, respectively. The number of induced morphologies with the film thicknesses of $H/L_0 = 1.0$ and $H/L_0 = 2.0$ is larger than that

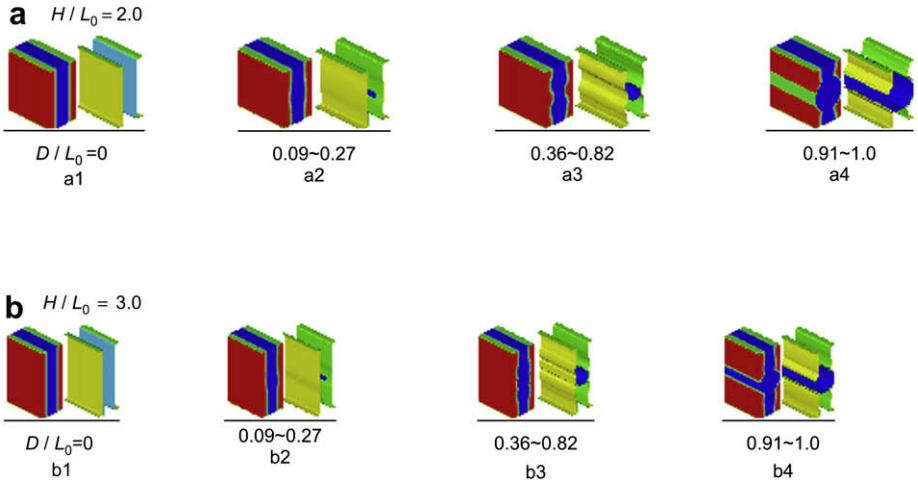

Fig. 2. Morphologies of symmetric DBCPs films with embedded one neutral NR. For different film thicknesses $H/L_0 = 2.0$ (a) and $H/L_0 = 3.0$ (b), the relative nanorod diameter D/L_0 increases from 0 to 1.0 in step of 0.09. The red domains are A blocks and the blue domains are B blocks. The blue poles in isodensity surfaces denote the NRs. (For interpretation of the references to color in this figure legend, the reader is referred to the web version of this article.)

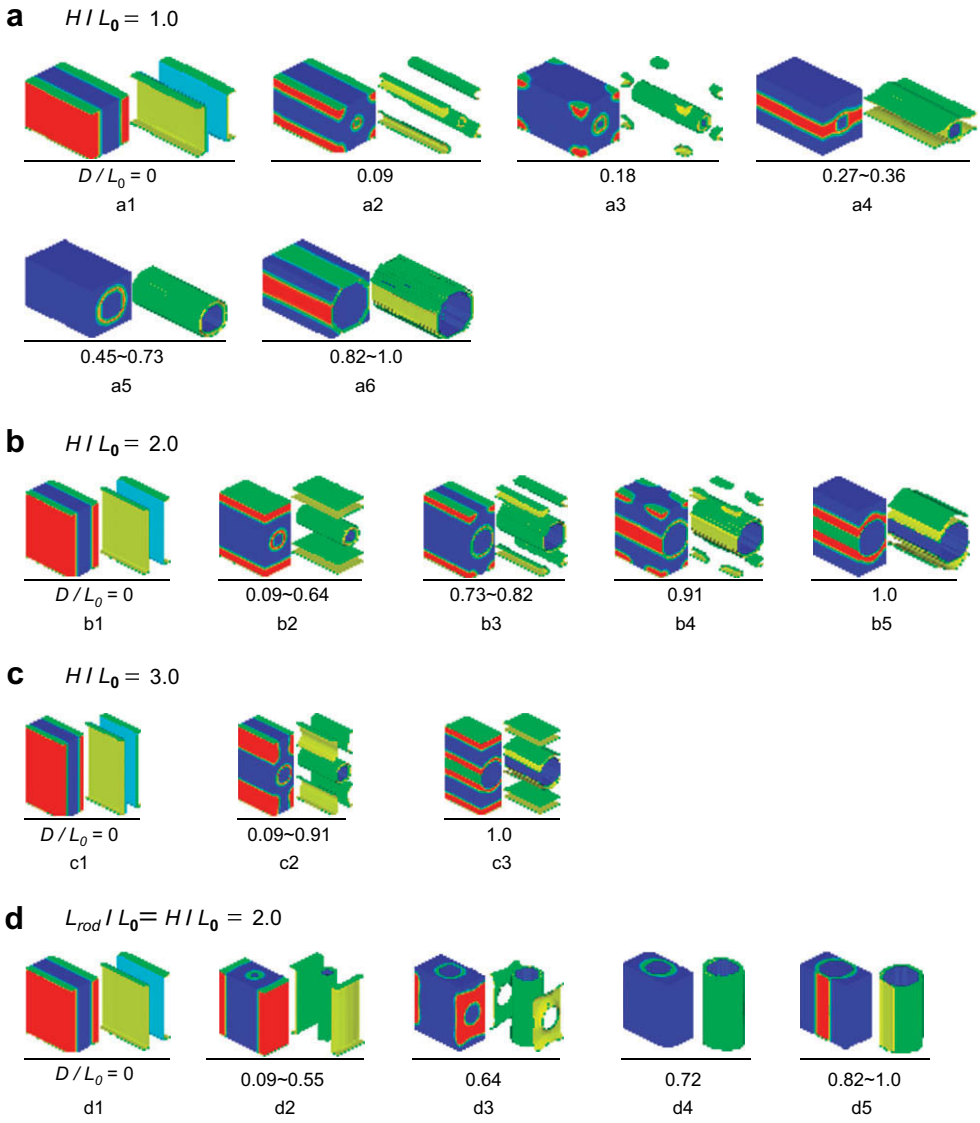

Fig. 3. Morphologies of symmetric DBCPs films with embedded one A-attractive nanorod. The relative nanorod diameter D/L_0 increases from 0 to 1.0 in step of 0.09. For the NR arranged in the *y*-direction with different film thicknesses $H/L_0 = 1.0$ (a), $H/L_0 = 2.0$ (b), and $H/L_0 = 3.0$ (c), for the NR arranged in the z direction with finite length $L_{rod}/L_0 = H/L_0 = 2.0$ (d), here, L_{rod} represents the NR length.

of $H/L_0 = 3.0$, which indicates the fact that induced structures of symmetric DBCPs confined films with embedded one A-attractive NR are not only sensitive to nanorod diameter D but also to film thickness H. Obviously, these new self-assembled structures are formed from the cooperation between two parallel surfaces and NR. To explore further the effects of the inner-outer surface confinements, we discuss the self-assembly of symmetric diblocks with $H/L_0 = 2.0$ in detail. An increase in D/L_0 from 0.09 to 0.91 drives an induced transition from lamellar ($L_{\|}$) to incomplete cylindrical ($C_{1/2}$) and to incomplete spherical ($S_{1/2}$) phases near the film surfaces in Fig. 3(b2)–(b4), which is consistent with that of diblock copolymers A_nB_m in the bulk (i.e. the value of f_A reducing from 0.4 to 0.2). This result can be interpreted that when diblock copolymers are embedded with a small NR, only a few A blocks are strongly attracted to the nanorod forming the "coating", and the effective symmetry in block composition is still kept, and this promotes the formation of lamellar structure ($L_{\|}$), see (b2). Then, with the increase of D/L_0, some A blocks are strongly attracted to the NR, and it equivalently reduces the effective A block composition (f_{eff}) in the remaining copolymers. This leads to promoting a transition from lamellar phase to cylindrical structure ($C_{1/2}$), see (b3). When the diameter of nanorod D increases again, the more A blocks are attracted to the NR. This leads the further reduction of effective A block composition (f_{eff}) in remaining copolymers, and promotes a transition from cylindrical phase to spherical structure ($S_{1/2}$), see (b4). However, due to the top and bottom surface confinements, we only observe incomplete cylindrical and spherical structures (i.e. $C_{1/2}$, $S_{1/2}$). The results also highlight the fact that the self-assembly of symmetric DBCPs melt is cooperatively induced by the inner and outer surface confinements. In our calculation, periodic boundary conditions are adopted. Therefore, if the length of nanorod is finite, nanorods are fixed and arranged in the *y*-direction, it is more difficult to deal with more than one nanorods in experiments. Thus, we present the results of the case that one NR with finite length L_{rod}, located in the center of *xy*-plane along *z* direction in Fig. 3d. Here, $L_{rod}/L_0 = H/L_0 = 2.0$. Similarly, due to the strong adsorption of nanorod to A block, there is also a central cylinders (C') consisting of the NR and A blocks. Besides the central cylinders (C'), the induced structures include $L_{\|}$ (d2) and *PL* (d3), where *PL* represents perforated.

In the experimental studies [58,59], the NRs are always mobile and have finite length. Therefore, it is more important in nanoscience to investigate the mesophases of the mixture of block copolymers and mobile NRs with finite length. However, although the self-consistent field (SCF) has proven to be a powerful method for calculating equilibrium morphologies, it is restricted and even incorrect to investigate the morphologies for the mixture of block copolymer melts and mobile nanoparticles/nanorods. To study the mixture of block copolymer/mobile NR, one should use new modified SCF [52–54]. At the same time, dissipative particle dynamics (DPD) is one of the most effective method to study the effects of the nanorod length, the nanorod orientation, and the nanorod–polymer interaction on the morphologies for the mixture of block copolymer melts and mobile nanorods. However, in this report, our aim is to study cooperative surface-induced self-assembly of symmetric diblock copolymers with different inner and outer confinements such as DBCPs confined in-between two concentric spheres with radii R_1 and R_2 [60]. Therefore, although such simulations are difficult to correspond to the real system in experiments, the result is helpful to the researchers to understand the self-assembly mechanism of composited block copolymer system with nanorods [60].

To understand comprehensively the cooperative inducement of two parallel surfaces and the nanorod to self-assembly of symmetric DBCPs, we construct a phase diagram for symmetric DBCPs with embedded one A-attractive nanorod as plotted in Fig. 4. Here, the film thickness H/L_0 increases from 1.0 to 3.0, and nanorod diameter D/L_0 increases from 0 to 1.0. In this phase diagram, graphic symbols represent the morphologies given at the bottom of Fig. 4. For example, for the cases of $D/L_0 = 0.18$, 0.45 and 0.91, when H/L_0 increases, the confinement-induced structure transitions can be expressed as $S_{1/2}+C'\rightarrow C_{1/2}+C'\rightarrow L_{\|}+C'\rightarrow C_{1/2}+C', L_{\|}+C'\rightarrow S_{1/2}+C'\rightarrow C_{1/2}+C'\rightarrow L_{\|}+C'\rightarrow C_{1/2}+C'$, and $C'\rightarrow S_{1/2}+C'\rightarrow C_{1/2}+C'\rightarrow L_{\|}+C'\rightarrow C_{1/2}+C'$. There is the same transition $(S_{1/2}+C'\rightarrow C_{1/2}+C'\rightarrow L_{\|}+C'\rightarrow C_{1/2}+C')$ in the three cases. It is shown that the induced phase structures with different film thicknesses $H/L_0$and nanorod diameters D/L_0 have some regularity on the whole. In addition, we count the A/B block composition (f_A and f_B) in final morphologies. The ratio of f_A/f_B is equal to 1.0, even for large nanorods (i.e. $D/L_0 > 0.8$).

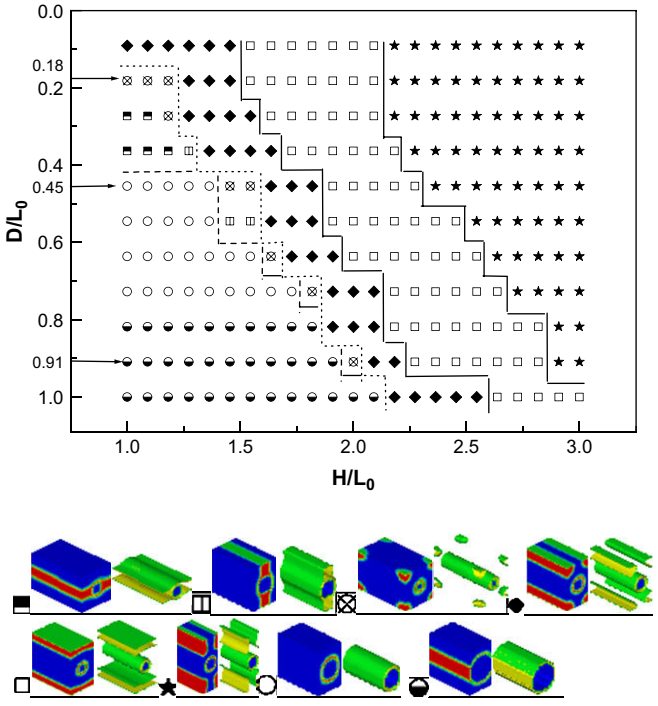

Fig. 4. The phase diagram for symmetric DBCPs films with embedded one A-attractive NR. Graphic symbols present simulation points, while lines serve as guide to eye. ■ = $L_{//}+C'$, ◫ = $L_{\perp}+C'$, ⊠ = $S_{1/2}+C'$, ◆ = $C_{1/2}+C'$, □ = $L_{//}+C'$, ★ = $C_{1/2}+C'$, ○ = C', and ◒ = C'.

3.2. Two nanorods

We now consider the morphologies for diblocks with embedded two nanorods (NRs), and the model is shown in Fig. 1(c)–(d), respectively. Fig. 5 shows the results for two neutral NRs with the film thicknesses of $H/L_0 = 2.0$ and $H/L_0 = 3.0$. When the diameter of D/L_0 increases, it is also observed that the neutral NRs have almost no effect on the perpendicular lamellae ($L_{\perp}$) of symmetric DBCPs confined films.

When two A-attractive NRs are embedded in diblocks in the period of one lamellae, the results are similar to that of one NR. Except for two central cylinders (C'), formed by two NRs and the "coating" consisting of A blocks, some new induced structures are also observed in Fig. 6, which cannot be obtained in neat symmetric DBCPs confined films. When $H/L_0 = 2.0$, $H/L_0 = 3.0$ and $H/L_0 = 4.0$, with increasing D/L_0 from 0 to 1.0, a series of integrated morphologies transitions of mixtures are predicted as:

$$L_{\perp}\rightarrow C_{1/2}+C+C'\rightarrow S+C'\rightarrow L_{\|}+C'\rightarrow C'\rightarrow C'$$

$$L_{\perp}\rightarrow C_{1/2}+L_{\|}+C'\rightarrow C+C'\rightarrow L_{\perp}+C'\rightarrow C'\rightarrow C'$$

$$L_{\perp}\rightarrow L_{\|}+C'\rightarrow C_{1/2}+L_{\|}+C'\rightarrow S_{1/2}+C+C'\rightarrow C'$$

Except for the central cylinders (C'), these induced structures include mainly $C+C$ (a2), S (a3), $L_{//}$ (a4, c2), $C_{1/2}+L_{//}$ (b2, c3), C (b3), $L_{\perp}$ (b4) and $S_{1/2}+C_{1/2}$ (c4), where C, S, $L_{//}$ and $L_{\perp}$ represent the morphologies of cylinder, sphere, parallel and perpendicular lamellae, respectively. To explore further how the film thickness H and nanorod diameter D affect the self–assembled structures of symmetric DBCPs, we consider the results of $H/L_0 = 4.0$ in detail. Similarly, near the film surfaces, an increase in D/L_0 from 0.09 to 0.91 drives an induced structure transition from lamellar ($L_{//}$) to incomplete cylindrical ($C_{1/2}$), and to incomplete spherical ($S_{1/2}$) phases in Fig. 6 (c2)–(c4), which is consistent with that of diblock copolymers A_nB_m in the bulk (i.e. value of f_A decreasing from 0.4 to 0.2). These induced structures can also be interpreted that through increasing nanorod diameter D, some A blocks are strongly attracted to NRs, and it equivalently reduces the effective A block composition (f_{eff}) in remaining copolymers. This leads one to have the phase structure transitions from lamellar ($L_{//}$) to incomplete

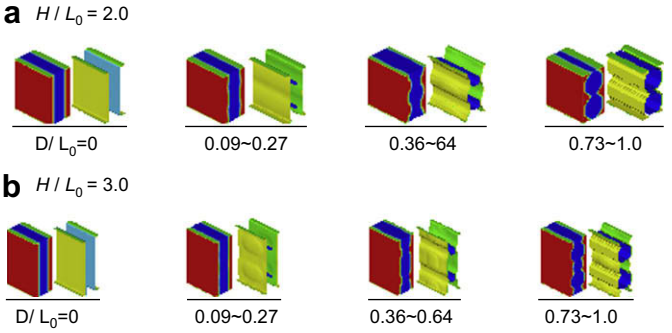

Fig. 5. Morphologies of symmetric DBCPs films with embedded two neutral NRs. For different film thicknesses H/L_0 = 2.0 (a) and $H/L_0 = 3.0$ (b), the relative nanorod diameter D/L_0 increases from 0 to 1.0 in step of 0.09.

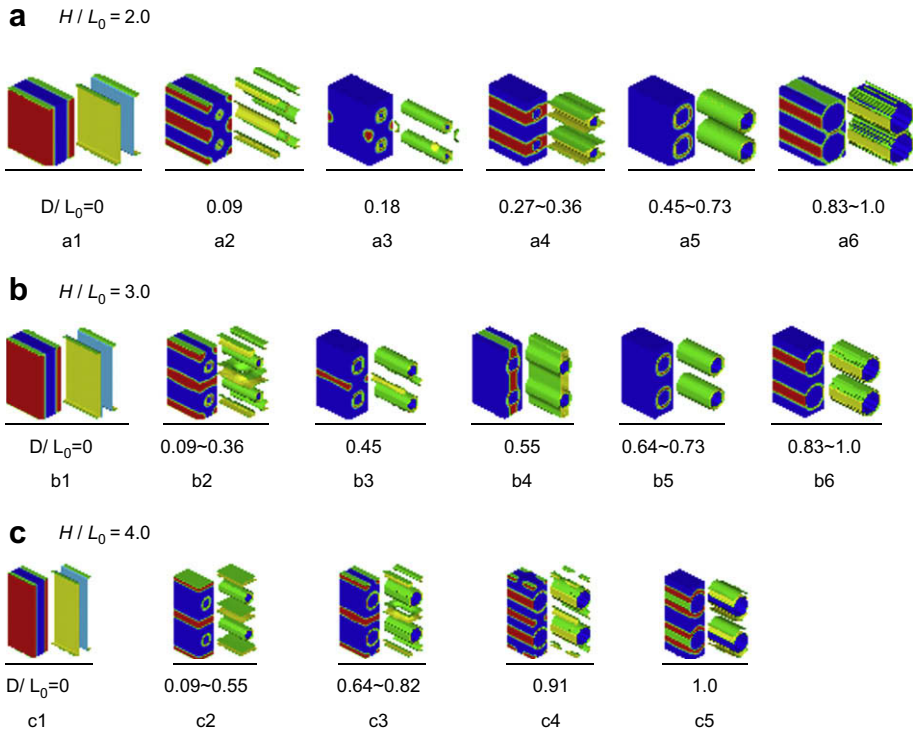

Fig. 6. Morphologies of symmetric DBCPs films with embedded two A-attractive NRs. For different film thicknesses $H/L_0 = 2.0$ (a), $H/L_0 = 3.0$ (b), and $H/L_0 = 4.0$ (c), the relative nanorod diameter D/L_0 increases from 0 to 1.0 in step of 0.09.

cylindrical ($C_{1/2}$), and then to incomplete spherical ($S_{1/2}$) phases. Likewise, due to the inner surface confinement from top and bottom surfaces, there are only incomplete cylindrical and spherical structures (i.e. $C_{1/2}$, $S_{1/2}$) observed near the film surfaces.

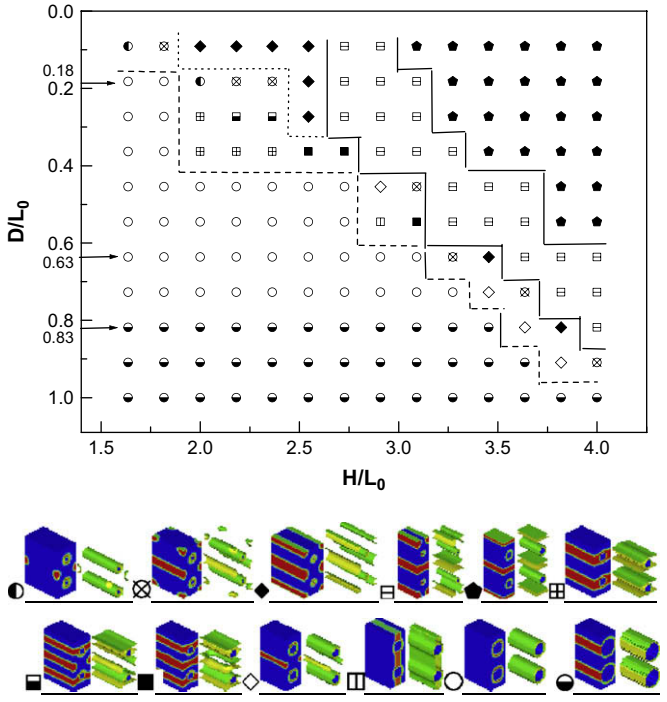

Fig. 7. The phase diagram for symmetric DBCPs films with embedded two A-attractive NRs. Graphic symbols represent simulation points, while lines serve as guide to eye. ◐ = $S + C'$, ⊠ = $S_{1/2} + C + C'$, ◆ = $C_{1/2} + C + C'$, ⊟ = $C_{1/2} + L_{//} + C'$, ⬟ = $L_{//} + C'$, ⊞ = $L_{//} + C'$, ⬓ = $C + L_{//} + C'$, ■ = $L_{//} + C'$, ◇ = $C + C'$, ◫ = $L_{\perp} + C'$, ○ = C' and ◒ = C'.

Surprisingly, there are also complete lamellar ($L_{//}$, c2), cylindrical (C, b3) and spherical (S, a3) structures formed at the interior of the films. Hence, the induced morphologies with two NRs are much richer than that of system containing one NR mentioned above.

We now combine our results for different values of H/L_0 and D/L_0 to sketch a phase diagram as shown in Fig. 7. For the given values of $D/L_0 = 0.18$, 0.63 and 0.83, with the increase of H/L_0, the confinement-induced structure transitions can be expressed as $C' \rightarrow S + C' \rightarrow S_{1/2} + C + C' \rightarrow C_{1/2} + C + C' \rightarrow C_{1/2} + L_{\|} + C' \rightarrow L_{\|} + C'$, $C' \rightarrow S_{1/2} + C' \rightarrow S_{1/2} + C + C' \rightarrow C_{1/2} + C + C' \rightarrow C_{1/2} + L_{\|} + C' \rightarrow L_{\|} + C'$ and $C' \rightarrow C + C' \rightarrow C_{1/2} + C + C' \rightarrow C_{1/2} + L_{\|} + C'$, respectively. There is the same underlined transition ($C_{1/2} + C + C' \rightarrow C_{1/2} + L_{\|} + C'$) in the three cases. Meanwhile, lines in phase diagram serve as guide to eye and make out the range of various morphologies regions. To some extend, the induced phase structures of the melt for different film thicknesses $H/L_0$and nanorod diameters D/L_0 show some regularity.

4. Conclusions

We studied the self-assembled structures of symmetric diblock copolymers (DBCPs confined films with embedded one or two nanorods (NRs) using the self-consistent field (SCF) theory. The NRs are neutral or preferential to one of blocks. For neutral NRs, it has almost no effect on the morphology of symmetric DBCPs confined films. By contrast, it is quite different for the case of A-attractive NRs. By changing film thickness H and nanorod diameter D, except for the central cylinders (C'), we observe various induced structures, such as lamellar ($L_{//}$), incomplete cylindrical ($C_{1/2}$) and incomplete spherical ($S_{1/2}$) phases, which do not exist in neat symmetric DBCPs confined films. It is interesting to note that an increase in nanorod diameter D leads one to have an induced structure transition from lamellar ($L_{//}$) to incomplete cylindrical ($C_{1/2}$), and then to incomplete spherical ($S_{1/2}$) phases. In fact, the increase of preferential nanorod diameter D equivalently changes the

effective block composition (f_{eff}) in remaining copolymers, and this leads one to form the induced structures (i.e. cylindrical and spherical phases). However, due to the coexistence of the inner confinement of two parallel surfaces, there are only incomplete cylindrical and spherical structures (i.e. $C_{1/2}$, $S_{1/2}$) observed near top and bottom surfaces. Surprisingly, for two preferential NRs, we also predict the existence of complete lamellar ($L_{//}$), cylindrical (C) and spherical (S) structures formed in the interior. As a result, it shows that these striking self-assembled structures are formed from cooperative inducement of both inner confinement (two parallel surfaces) and outer confinement (nanorods). Although it is difficult to obtain the nanorods embedded in diblocks in experiments yet now, this theoretical investigation helps us to understand the morphologies under complex confinements.

Acknowledgments

This research was financially supported by National Natural Science Foundation of China (Nos. 20574052, 20774066, 20525416), the National Basic Research Program of China (No. 2005CB623800), Program for New Century Excellent Talents in University (NCET-05-0538) and Natural Science Foundation of Zhejiang Province (Nos. R404047, Y4080098). We also thank the referees for their critical reading of the manuscript and their very good ideas.

References

[1] Hamley IW. The physics of block copolymers. Oxford: Oxford Science Publications; 1998.
[2] Matsen MW, Bates FS. Macromolecules 1996;29:1091.
[3] Matsen MW, Schick M. Phys Rev Lett 1994;72:2660.
[4] Zhang MQ, Rong MZ. Chin J Polym Sci 2003;21:587.
[5] Onuki A. Phase transition dynamics. Cambridge: Cambridge University Press; 2002.
[6] Harrison C, Adamson DH, Cheng Z, Sebastian JM, Sethuraman S, Huse DA, et al. Science 2000;290:1558.
[7] Rockford L, Mochrie SGJ, Russell TP. Macromolecules 2001;34:1487.
[8] Cheng JY, Mayes AM, Ross CA. Nat Mater 2004;3:823.
[9] Kim SO, Solak HH, Stoykovich MP, Ferrier NJ, dePablo JJ, Nealey PF. Nature (London) 2003;424:411.
[10] Hamley IW. Curr Opin Colloid Interface Sci 2000;5:342.
[11] Morrison FA, Winter HH, Gronski W, Barnes JD. Macromolecules 1990;23:4200.
[12] Chen ZR, Kornfield JA, Smith SD, Grothaus JT, Satkowski MM. Science 1997;277:1248.
[13] Morkved TL, Lu M, Urbas AM, Ehrichs EE, Jaeger HM, Mansky P, et al. Science 1996;273:931.
[14] Thurn-Albrecht T, DeRouchey J, Russell TP, Kolb R. Macromolecules 2002;35:8106.
[15] Boeker A, Knoll A, Elbs H, Abetz V, Mueller AHE, Krausch G. Macromolecules 2002;35:1319.
[16] Fasolka MJ, Mayes AM. Annu Rev Mater Res 2001;31:323.
[17] Knoll A, Lyakhova KS, Horvat A, Kraush G, Sevink GJA, Zvelindovsky AV. Nat Mater 2004;3:886.
[18] Krausch G, Magerle R. Adv Mater 2002;14:1579.
[19] Tsarkova L, Knoll A, Krausch G, Magerle R. Macromolecules 2006;39:3608.
[20] Yang Y, Qiu F, Zhang H, Yang Y. Polymer 2006;47:2205.
[21] Huinink HP, van Dijk MA, Brokken-Zijp JCM, Sevink GJA. Macromolecules 2001;34:5325.
[22] Pereira GG. J Chem Phys 2002;117:1878.
[23] Wang Q, Nealey PF, de Pablo JJ. Macromolecules 2001;34:3458.
[24] Wang Q, Yan Q, Nealey PF, de Pablo JJ. J Chem Phys 2000;112:450.
[25] Wu Y, Cheng G, Katsov K, Sides SW, Wang J, Tang J. Nat Mater 2004;3:816.
[26] Sevink GJA, Zvelindovsky AV. Macromolecules 2005;38:7502.
[27] Tang P, Qiu F, Zhang H, Yang Y. Phys Rev E 2005;72:016710.
[28] Feng J, Ruckenstein E. Macromolecules 2006;39:4899.
[29] Li W, Wickham RA, Garbary RA. Macromolecules 2006;39:806.
[30] Yu B, Sun P, Chen T, Jin Q, Ding D, Li B, et al. Phys Rev Lett 2006;96:138306.
[31] Chen P, He X, Liang H. J Chem Phys 2006;124:104906.
[32] Li W, Wickham RA. Macromolecules 2006;39:8492.
[33] Chen P, Liang H, Shi AC. Macromolecules 2007;40:7329.
[34] Wang Q. J Chem Phys 2007;126:024903.
[35] Yu B, Sun P, Chen T, Jin Q, Ding D, Li B, et al. J Chem Phys 2007;127:114906.
[36] Chantawansri TL, Bosse AW, Hexemer A, Ceniceros HD, Garcia-Cervera CJ, Kramer EJ, et al. Phys Rev E 2007;75:031802.
[37] Yu B, Li B, Jin Q, Ding D, Shi AC. Macromolecules 2007;40:9133.
[38] Xiang H, Shin K, Kim T, Moon S, McCarthy TJ, Russell TP. J Polym Sci Part B Polym Phys 2005;43:3377.
[39] Huang E, Russell TP, Harrison C, Chaikin PM, Register RA, Hawker CJ, et al. Macromolecules 1998;31:7641.
[40] Huang E, Rockford L, Russell TP, Hawker CJ. Nature (London) 1998;395:757.
[41] Busch P, Posselt D, Smilgies DM, Rheinlander B, Kremer F, Papadakis CM. Macromolecules 2003;36:8717.
[42] Frischknecht AL, Curro JG, Frink LJ. J Chem Phys 2002;117:10398.
[43] Walton DG, Kellogg GJ, Mayes AM. Macromolecules 1994;27:6225.
[44] Yin YH, Sun PC, Chen TH, Li BH, Jin QH, Ding DT. Chem Phys Chem 2004;5:540.
[45] Geisinger T, Muller M, Binder K. J Chem Phys 1999;111:5241.
[46] He X, Song M, Liang H, Pan C. J Chem Phys 2001;114:10510.
[47] Feng J, Liu H, Hu Y. Macromol Theory Simul 2002;11:549.
[48] Wang Q, Nealey PF, de Pablo JJ. J Chem Phys 2003;118:11278.
[49] Liu D, Zhong C. Macromol Rapid Commun 2006;27:458.
[50] Huh J, Ginzburg VV, Balazs AC. Macromolecules 2000;33:8085.
[51] Barrat J, Fredrickson GH. J Chem Phys 1991;95:1281.
[52] Thompson RB, Ginzburg VV, Matsen MW, Balazs AC. Science 2001;292:2469.
[53] Thompson RB, Ginzburg VV, Matsen MW, Balazs AC. Macromolecules 2002;35:1060.
[54] Lee JY, Thompson RB, Jasnow D, Balazs AC. Macromolecules 2002;35:4855.
[55] Sides SW, Kim BJ, Kramer EJ, Fredrickson GH. Phys Rev Lett 2006;96:250601.
[56] He L, Zhang L, Liang H. J Phys Chem B 2008;112:4194.
[57] Buxton GA, Balazs AC. Mol Simul 2004;30:249.
[58] Laicer CST, Chastek TQ, Lodge TP, Taton TA. Macromolecules 2005;38:9749.
[59] Laicer CST, Mrozek RA, Taton TA. Polymer 2007;48:1316.
[60] Marco P, Guo XH, Zvelindovsky AV. Polymer 2008;49:2797.
[61] Zhang QL, Gupta S, Emrick T, Russell TP. J Am Chem Soc 2006;128:3898.
[62] Sevink GJA, Zvelindovsky AV, van Vlimmeren BAC, Maurits NM, Fraaije JGEM. J Chem Phys 1999;110:2250.